Hindawi Publishing Corporation
Journal of Nanomaterials
Volume 2014, Article ID 821706, 7 pages
http://dx.doi.org/10.1155/2014/821706

Research Article

Controlled Synthesis of Water-Soluble $NaYF_4:Yb^{3+}$, Er^{3+} Nanoparticles with Surfactant Dependent Properties

Junwei Zhao,[1] Tiekun Jia,[1] Xiaofeng Wang,[1] and Xianggui Kong[2]

[1] *Department of Materials Science and Engineering, Luoyang Institute of Science and Technology, Luoyang 471023, China*
[2] *State Key Laboratory of Luminescence and Applications, Changchun Institute of Optics, Fine Mechanics and Physics, Chinese Academy of Sciences, Changchun 130033, China*

Correspondence should be addressed to Junwei Zhao; jwzhao2010@lit.edu.cn and Xianggui Kong; xgkong2000@163.com

Received 31 December 2013; Revised 5 March 2014; Accepted 6 March 2014; Published 31 March 2014

Academic Editor: Marinella Striccoli

Water-soluble $NaYF_4:Yb^{3+}$, Er^{3+} nanoparticles (NPs) are successfully prepared by a solvothermal reaction using branched polyethylenimine (PEI) with different chain lengths as the surfactants in a water/diethylene glycol (DEG) mixed solution. It is shown that the size of $NaYF_4$ NPs prepared with high molecular weight PEI (HPEI) is smaller than that of the NPs prepared with low molecular weight (LPEI), while small-sized NPs exhibit more intense upconversion luminescence intensities than large-sized NPs in the same excitation power of 980 nm. It is found that HPEI is conducive to the formation of smaller NP with high crystallinity. Small-sized $NaYF_4:Yb^{3+}$, Er^{3+} NPs with intense upconversion luminescence and improved crystallinity were related to their growth process. A possible growth mechanism of the samples is proposed. The results of this study can provide new insights into the controlled synthesis of novel NPs.

1. Introduction

In recent years, the upconversion luminescence of rare-earth fluoride NPs has attracted great research interest of the research groups in the world due to their potential applications in various fields, such as photodetectors and fluorescent labels or imaging probes [1–7]. Compared with downconversion fluorescent nanomaterials, upconversion luminescence NPs have many conceivable advantages in the field of biomedicine [8–10]. The upconversion luminescence nanomaterials have achieved considerable results, but many biomedicine experiments are still proof of concept [11]. In order to carry out their widespread application in biomedical fields, the upconversion luminescence NPs should be small enough and water soluble and exhibit high fluorescent intensity. Synthesis of upconversion luminescence nanomaterials with high crystal quality, uniform particle size distribution, and adjustable spectrum is still a challenge. Fluoride matrix materials show some unique advantages because of their low phonon frequencies observed in the crystal lattice [12]. Rare-earth ion-doped fluoride under 980 nm near-infrared (NIR) excitation can reduce the multiphonon relaxation process; thereby activating ions have a long-lived excited state, improving the luminescence intensity of the materials. So far, $NaYF_4$ has been considered the most effective matrix for upconversion luminescence [3, 12]. Therefore, it is important to develop efficient and convenient methods to synthesize $NaYF_4$:Yb, Er NPs with high quality and monodispersion for various biomedical applications.

Over the past few years, many research groups have made great efforts to explore the feasible synthesis methods of upconversion luminescence NPs. Many chemical synthesis technologies, including coprecipitation [13–15], thermal decomposition [16–18], and hydrothermal synthesis [19, 20], have been demonstrated to synthesize lanthanide-doped upconversion luminescence NPs. However, most of these synthesized methods of NPs are in an organic solvent or at high temperature and usually require heat after treatment or produce toxic byproducts [1]. In our previous work, we have used ethylenediaminetetraacetic acid disodium salt (EDTA) and sodium citrate as the surfactants to synthesize $NaYF_4$ NPs [21, 22]; however, these NPs are difficult to disperse in water for a long time due to the lack of sufficient hydrophilic groups on the NP surface.

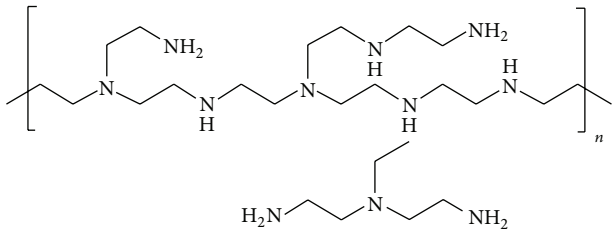

Figure 1: The molecular structure of branched PEI.

In this work, water-soluble $NaYF_4$:Yb^{3+}, Er^{3+} NPs are successfully prepared via a solvothermal method using branched PEI with different chain lengths as the surfactants. The influence of surfactant chain length on the size, crystallinity, and upconversion luminescence of $NaYF_4$:Yb^{3+}, Er^{3+} NPs was discussed in detail. All the obtained NPs exhibit strong upconversion fluorescence under 980 nm excitation. A possible growth mechanism of the samples is proposed. These nanocrystals have great potential for use in biology and medicine as fluorescent labels or imaging probes.

2. Experimental Section

2.1. Materials. All reagents were of analytical grade. $Ln(NO_3)_3{\cdot}6H_2O$ (Ln = Y, Yb, and Er) stock solution was freshly prepared by the reaction of Ln_2O_3 with dilute nitric acid. Deionized water was prepared using a Millipore Milli-Q Purification System; its resistivity is more than 18.2 MΩ. The different molecular weight PEI polymers were purchased from Sigma-Aldrich. The molecular structure of PEI is shown in Figure 1. PEI stock solution (5 wt%) was prepared by diluted PEI with deionized water.

2.2. Synthesis of Water-Soluble $NaYF_4$:Yb^{3+}, Er^{3+} NPs. In a typical procedure for the preparation of $NaYF_4$: 20 mol% Yb^{3+}, 2 mol% Er^{3+} NPs, a PEI solution (5 mL, 5 wt%) was added to a mixture of $Ln(NO_3)_3{\cdot}6H_2O$ aqueous solution (2.5 mL, 0.2 mol/L, lanthanide ion molar ratio, and Y/Yb/Er = 78 : 20 : 2), NaCl aqueous solution (2.5 mL, 0.2 mol/L), and DEG (20 mL) with vigorous stirring for 1 h. An aqueous solution of NH_4F was then added slowly to the above mixture with vigorous stirring for 1 h and the pH value of the system was adjusted to 7.5 using NaOH and HCl solutions. Then the prepared precursor solution was transferred to a 50 mL autoclave with polytetrafluoroethylene lining. The reaction autoclave was placed in a digital type heating furnace to heat to 180°C temperature and maintained at the temperature for several hours before natural cooling to room temperature. Finally, $NaYF_4$:Yb^{3+}, Er^{3+} precipitation can be separated out by centrifugation (6500 rpm, 10 min). The separated precipitation was washed with deionized water and ethanol for three times, respectively. The obtained $NaYF_4$:Yb^{3+}, Er^{3+} NPs were dried in vacuum at 60°C for 24 hours.

2.3. Characterization. The structure and morphology of $NaYF_4$:Yb^{3+}, Er^{3+} NPs were characterized by means of X-ray powder diffractometer (XRD), scanning electron microscopy (SEM, Hitachi, S-4800), and the Fourier transform infrared (FT-IR) spectra (Perkin-Elmer 580B infrared spectrophotometer). The operation voltage and the current of a Brucker D8-advance X-ray diffractometer with CuKα radiation (λ = 1.5418 Å) when testing the samples were 40 kV and 40 mA, respectively. The 2θ angle ranges from 15 to 60° with step of 0.021 and counting time of 0.2 s. All parameters during XRD data collection were kept constant. The upconversion emission spectra of $NaYF_4$:Yb^{3+}, Er^{3+} phosphors were acquired using a Jobin-Yvon LabRam Raman spectrometer system equipped with 1800 and 600 grooves/mm holographic gratings, respectively, and a Peltier air-cooled CCD detector. The dry powder samples were excited by a CW semiconductor diode laser at 980 nm. The maximal excitation power used in the experiment was about 760 mW with a focusing area of about 0.03 mm^2. The upconversion luminescence spectra were measured under identical conditions in order to compare their relative emission intensities.

Table 1: The synthesis conditions and characteristics of the samples prepared via the solvothermal method.

Sample number	Molecular weight	Solvothermal time (h)	Sample size (nm)
L1	2000	3 h	58 nm
L2	2000	5 h	64 nm
H1	25000	3 h	40 nm
H2	25000	5 h	45 nm

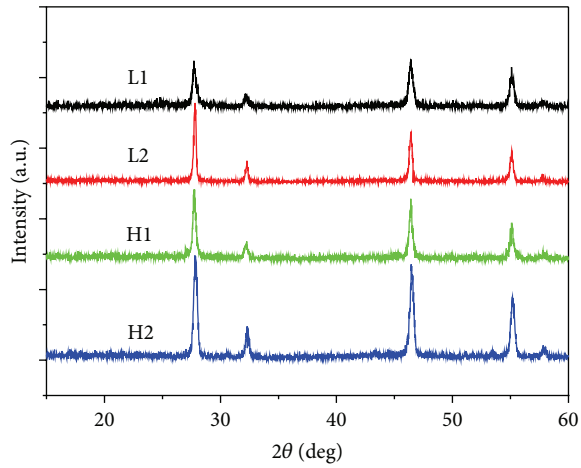

Figure 2: XRD patterns of the as-prepared samples. All the samples are prepared under the conditions according to Table 1.

3. Results and Discussion

3.1. Structure and Morphology. In order to study the molecular weight of PEI on the effect of sample, we on purpose synthesized four samples using different synthetic conditions. The synthetic conditions and characteristics of samples prepared via the solvothermal route are listed in Table 1. The structure and crystallinity of the products were characterized by XRD. Figure 2 shows the XRD patterns of the $NaYF_4$: 20 mol% Yb^{3+}, 2 mol% Er^{3+} NPs prepared with different

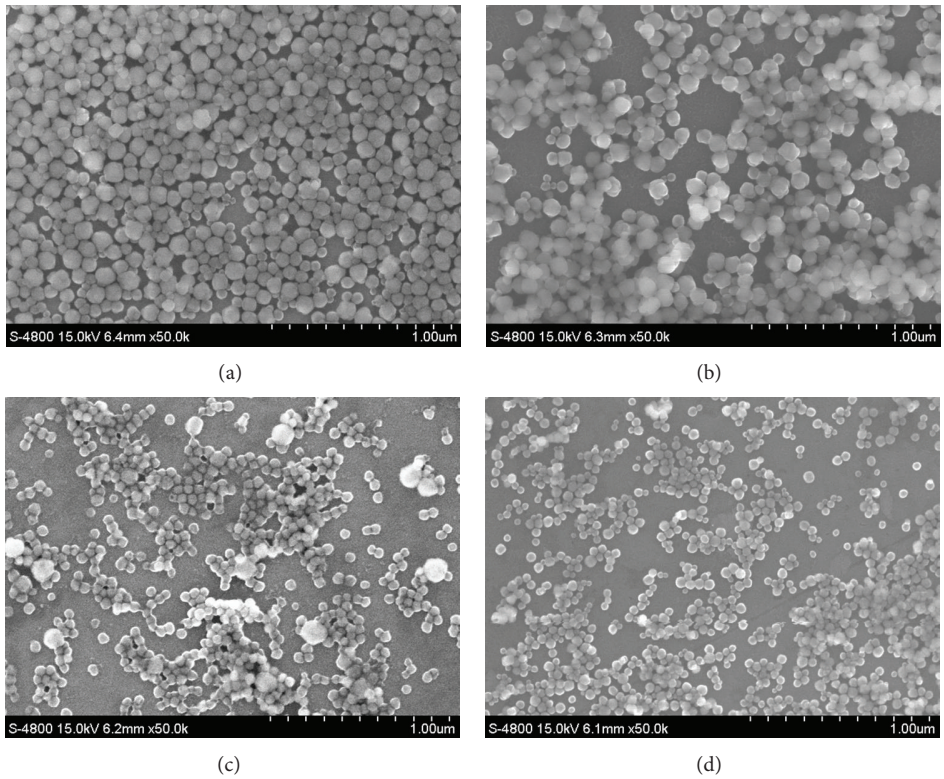

(a) (b) (c) (d)

Figure 3: SEM images of the $NaYF_4$: 20 mol% Yb^{3+}, 2 mol% Er^{3+} NPs prepared under different conditions: (a) LPEI, 3 h; (b) LPEI, 5 h; (c) HPEI, 3 h; (d) HPEI, 5 h.

solvothermal time using HPEI and LPEI, respectively. As can be seen from Figure 2, all diffraction peaks of the four samples coincide with the standard face-centered cubic structure data (JCPDS card number 77-2042). No additional diffractions of impurities are observed. Assuming a homogeneous strain across crystallites, the average size of microcrystallites can be estimated from the full width half maximum (FWHM) values of diffraction peaks using the Debye-Scherrer formula [23]. The average sizes of the samples L1, L2, H1, and H2 are 58 nm, 64 nm, 40 nm, and 45 nm, respectively. The diffraction peaks of the as-prepared samples show different intensity. After treatment of the precursors under the same solvothermal conditions, the intensity of the XRD diffractograms of the NPs synthesized with HPEI is stronger and the particle size is smaller, compared with that of the NPs synthesized with LPEI. The different intensity of the XRD diffractograms of the four samples should be related to their different crystallinity. This is similar to the results previously published for synthesis of anatase Titania using the hydrothermal technique [24].

Figure 3 shows the SEM images of the $NaYF_4$: 20 mol% Yb^{3+}, 2 mol% Er^{3+} NPs prepared according to the synthesis conditions in Table 1. As can be seen from Figure 3, the NPs synthesized with LPEI exhibited a spherical shape with an average size of about 60 nm. The NPs exhibit rough surface and nonuniform size distribution (see Figures 3(a) and 3(b)), which represent a low degree of crystallinity [21]. On using HPEI, the size of the obtained NPs with regular shape and uniform size is about 42 nm. When the solvothermal time reached 5 h, the crystallinity of the $NaYF_4$ NPs was further improved, as evidenced by the more regular shape and the smoother surface (see Figure 3(d)). Moreover, the size of the NPs prepared with HPEI is smaller than that of the NPs prepared with LPEI via the same solvothermal treatment process. The average size estimated from the SEM images is in agreement with the estimated value from the XRD patterns. The XRD spectrum data and the SEM image data complement each other well.

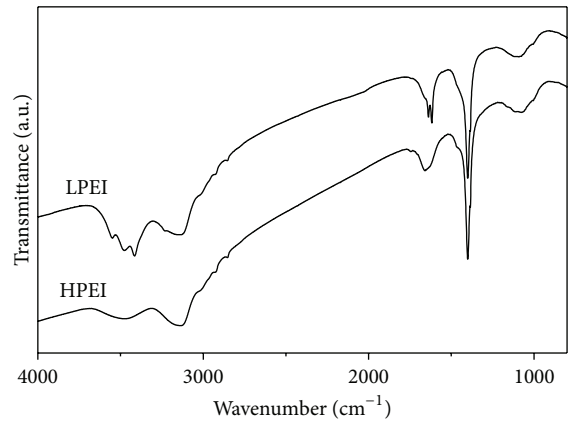

Figure 4: FT-IR spectra of the $NaYF_4$:Yb^{3+}, Er^{3+} NPs.

Figure 4 shows the FT-IR spectra of the $NaYF_4$:Yb^{3+}, Er^{3+} NPs. The strong absorption bands at 3500 and 3300 cm^{-1} of

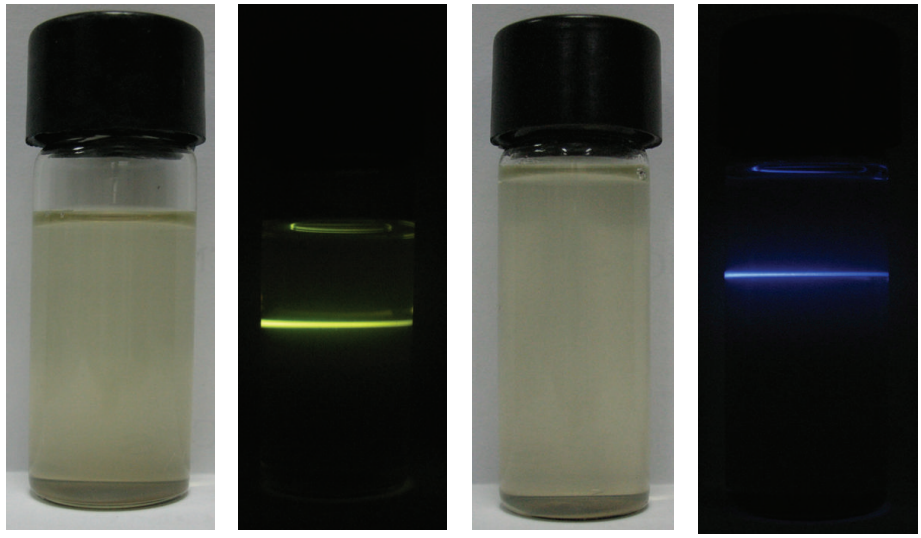

Figure 5: The photographs of the as-prepared $NaYF_4$:Yb^{3+}, Er^{3+}/Tm^{3+} NPs (sample H2) dispersed in aqueous solution under white light and 980 nm excitation.

the $NaYF_4$:Yb^{3+}, Er^{3+} NPs are the result of the NH vibrations [25]. The weak absorption bands of 2928 and 2853 cm^{-1} result from the asymmetrical and symmetrical stretching vibration of the CH_2 groups, respectively [26]. The absorption bands of 1650 and 1550 cm^{-1} are attributed to in-plane vibrations of the NH bonds [25]. The peaks at about 1450 cm^{-1} arised from vibrations of the C–C groups [26]. The presence of free amine groups on the surface of the nanoparticles is of extreme importance since these can bond with the ligand molecule (e.g., antibody) necessary for additional functionalization of the nanoparticle. The obtained NPs can be dispersed in water for two weeks without obvious precipitation due to the presence of sufficient hydrophilic groups on the NP surface (see Figure 5).

3.2. Possible Growth Mechanism. As discussed above, the size of the $NaYF_4$ NPs synthesized with HPEI is smaller than that of the NPs synthesized with LPEI under the same solvothermal conditions. This can be understood from the growth mechanism of crystals. The process of precipitation from a liquid phase to a solid phase is inevitable when using wet chemical synthesis of bulk and NPs [27]. The formation process of NPs includes the production of the nucleation, growth, and final shaping. Therefore, in order to understand the intrinsic factors which influence the size of NPs, it is needed to start studying nucleation mechanism of NPs. For a solute, any solution has certain solubility; thereby the excess solute will inevitably lead to the occurrence of the precipitation and formation of a crystal in solution. Therefore, to obtain the NPs in solution, the solute must reach supersaturation and then the nucleation occurs. The nucleation rate is one of the key factors to determine the size of NPs. The high nucleation rate is conducive to the formation of small-sized NPs because their subsequent growth process can be hindered by the solution since the rapid nucleation consumes more reactants [21, 24]. In our case, the PEI-Ln complex in the initial stage begins to form; the incorporation of anions into the PEI-Ln complex has a significant effect on nucleation rate. In the nucleation stage the Ln ions which are released slowly from the PEI-Ln complex reacted with F anions, transferring them into the $NaYF_4$ crystal nucleuses. In our previous report, we have reported the effect of the difference of chelate constant between EDTA and sodium citrate on the nucleation rate and then the size of NPs [21]. However, the chelate constant or chelating ability of PEI is almost not influenced by the degree of polymerization [28]. In this work, the PEI surfactants with different chain lengths are composed of the same monomer. Therefore, the nucleation rate is almost the same since the weight percentage of HPEI in precursors is the same as that of LPEI. In other words, the effect of the nucleation rate was not the determinant of the size difference of the as-prepared NPs. The particle growth stages followed the nucleation process. When the solute concentration decreased to a critical level, the nucleation process is stopped and the particles continue to grow by adding the reactive ions until reaching a new equilibrium concentration of the precipitated species [27]. In the growth stage, crystal nuclei are to form the primary particles which serve as growth center of NPs [21]. The ions that continually diffuse to the surface of the growing crystal, subsequently, incorporate into the lattice structure. Therefore, the diffusion rate of ions is another key factor to control the size and shape of the growing crystal. In water/DEG solution, the diffusion rate of the ions was slow due to the high viscosity of DEG. It is a reason for the synthesis of small-sized NPs. However, the influence of water/DEG solution is almost exactly the same for the four samples because of the same solvent. On the other hand, it is more important that PEI molecules as chelating ligands were bonded with rare-earth ions to form the PEI-Ln complex which reduced the diffusion rate of cations in solution to deposit on crystal surfaces. The later conditions

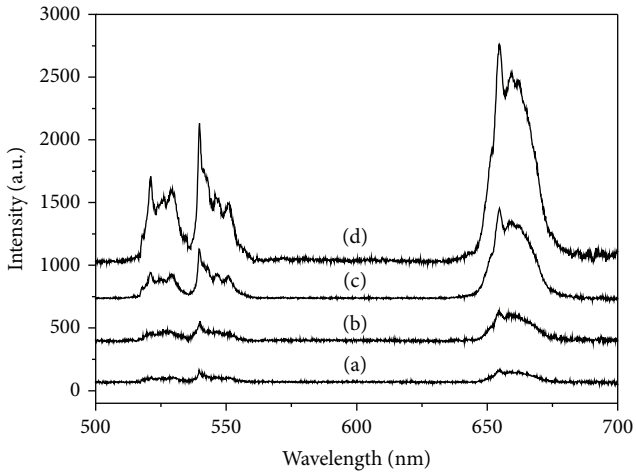

FIGURE 6: Upconversion luminescence spectra of the dried power $NaYF_4$:Yb^{3+}, Er^{3+} samples prepared with different solvothermal conditions according to Table 1 (λ_{ex} = 980 nm, power = 760 mW): (a) LPEI, 3 h; (b) LPEI, 5 h; (c) HPEI, 3 h; (d) HPEI, 5 h.

make the size difference possible during the growth of NPs. It is well known that the degree of polymerization of HPEI is higher than that of LPEI. The chain length of the HPEI like a tail is longer than that of LPEI. Therefore, the diffusion rate of the cations bound to HPEI molecules in solution is slower than that of the cations bound to LPEI molecules, with the result that the growth rate of the $NaYF_4$ NPs prepared with HPEI is slower than that of the NPs prepared with LPEI. Finally, the size of $NaYF_4$ NPs prepared with HPEI is smaller than that of the NPs prepared with LPEI. As we all know, ideal perfect crystals with well crystallinity would grow exceedingly slowly. That would be difficult to achieve since real crystals always have relatively few disruptions in their lattice structure. The only thing we can do is to reduce the crystallite defects to improve the crystal quality. During the growth stage, the slower the diffusion rate of ions is, the better the crystallinity is. Therefore, in this work the reason that the crystallinity of small-sized $NaYF_4$ seems to be higher than that of the biggest ones under the same solvothermal conditions is the slow growth rate of them.

In addition, the size of the as-prepared NPs is increasing with increasing solvothermal time when using the same molecular weight PEI molecules. It is reported that temperature has a certain influence on the stability of crystal nucleus [29]. As the crystal nucleus stability decreases, the nucleation rate of nonoxide crystals decreases with increasing the temperature [29]. As discussed above, the low nucleation rate leads to the increasing size of NPs. This is the reason that the particle size of obtained $NaYF_4$ NPs was increased with increasing the temperature.

3.3. Upconversion Photoluminescence of the $NaYF_4$:Yb^{3+}, Er^{3+} NPs. Figure 6 shows the upconversion photoluminescence spectra of the four dry powder samples prepared with different solvothermal conditions according to Table 1. Several distinct green and red emission bands centered at 520, 540, and 650 nm were observed. The green and red emission bands could be assigned to ($^2H_{11/2}$, $^4S_{3/2}$) $\rightarrow$ $^4I_{15/2}$ and $^4F_{9/2}$ $\rightarrow$ $^4I_{15/2}$ transitions of the Er^{3+} ions in the $NaYF_4$ NPs, respectively. In spite of the degree of polymerization of PEI, the relative upconversion luminescence intensity of samples under solvothermal treatment for 5 h is higher than that of samples under solvothermal treatment for 3 h, which is similar to the previous report [22]. Surprisingly, the upconversion luminescence intensity of the small-sized $NaYF_4$:Yb^{3+}, Er^{3+} NPs prepared with HPEI is stronger than that of the large-sized $NaYF_4$:Yb^{3+}, Er^{3+} NPs prepared with LPEI undergoing the same solvothermal treatment process. The observed phenomena are opposite to the common phenomenon. Generally, the NPs with large size exhibit the strong luminescence due to the reduced nonradiative relaxation [22, 30]. This opposite phenomenon in this research is probably related to the difference between HPEI and LPEI. The luminescence difference of samples prepared by different precursors has been reported in previous work [31, 32]. As discussed above, the PEI ligands influence the growth processes of the NPs. The difference in the chain length of PEI leads to a different diffusion rate. Therefore, it is suggested that the samples with the smallest size particle probably have the higher crystallinity because they exhibit the highest relative emission intensity.

4. Conclusions

Water-soluble $NaYF_4$:Yb^{3+}, Er^{3+} NPs are successfully prepared by a solvothermal reaction using PEI with different chain lengths as the surfactants in a water/DEG mixture. HPEI may favour the formation of small-sized NPs with a high degree of crystallinity. The size of $NaYF_4$:Yb^{3+}, Er^{3+} NPs prepared with HPEI is smaller than that of the NPs prepared with LPEI, while small-sized NPs exhibit more intense relative UC luminescence intensities than large-sized NPs under the excitation of 980 nm NIR light. It is suggested the upconversion luminescence properties and the improved crystallinity of small-sized NPs should be related to the growth process controlled by the chain length of PEI. The obtained NPs have great potential for use in biology and medicine as fluorescent labels or imaging probes.

Conflict of Interests

The authors declare that there is no conflict of interests regarding the publication of this paper.

Acknowledgments

This work was financially supported by the National Natural Science Foundation of China (Grant nos. 11204122 and U1304520), the Natural Science Research Project of the Education Department of Henan Province (Grant no. 12B430016), and the State Key Lab of Materials Synthesis and Processing of Wuhan University of Technology for the fund support.

References

[1] F. Wang and X. Liu, "Recent advances in the chemistry of lanthanide-doped upconversion nanocrystals," *Chemical Society Reviews*, vol. 38, no. 4, pp. 976–989, 2009.

[2] F. Wang, D. Banerjee, Y. Liu, X. Chen, and X. Liu, "Upconversion nanoparticles in biological labeling, imaging, and therapy," *Analyst*, vol. 135, no. 8, pp. 1839–1854, 2010.

[3] F. Auzel, "Upconversion and anti-stokes processes with f and d ions in solids," *Chemical Reviews*, vol. 104, no. 1, pp. 139–174, 2004.

[4] J. Zhou, X. J. Zhu, M. Chen, Y. Sun, and F. Y. Li, "Water-stable $NaLuF_4$-based upconversion nanophosphors with long-term validity for multimodal lymphatic imaging," *Biomaterials*, vol. 33, no. 26, pp. 6201–6210, 2012.

[5] A. Xia, M. Chen, Y. Gao, D. M. Wu, W. Feng, and F. Y. Li, "Gd^{3+} complex-modified $NaLuF_4$-based upconversion nanophosphors for trimodality imaging of NIR-to-NIR upconversion luminescence, X-Ray computed tomography and magnetic resonance," *Biomaterials*, vol. 33, no. 21, pp. 5394–5405, 2012.

[6] L. L. Li, R. B. Zhang, L. L. Yin et al., "Biomimetic surface engineering of lanthanide-doped upconversion nanoparticles as versatile bioprobes," *Angewandte Chemie*, vol. 51, no. 25, pp. 6121–6125, 2012.

[7] A. G. Zhou, Y. C. Wei, B. Y. Wu, Q. Chen, and D. Xing, "Pyropheophorbide A and c(RGDyK) comodified chitosan-wrapped upconversion nanoparticle for targeted near-infrared photodynamic therapy," *Molecular Pharmaceutics*, vol. 9, no. 6, pp. 1580–1589, 2012.

[8] D. K. Chatterjee, A. J. Rufaihah, and Y. Zhang, "Upconversion fluorescence imaging of cells and small animals using lanthanide doped nanocrystals," *Biomaterials*, vol. 29, no. 7, pp. 937–943, 2008.

[9] R. Abdul Jalil and Y. Zhang, "Biocompatibility of silica coated $NaYF_4$ upconversion fluorescent nanocrystals," *Biomaterials*, vol. 29, no. 30, pp. 4122–4128, 2008.

[10] S. F. Lim, R. Riehn, W. S. Ryu et al., "In vivo and scanning electron microscopy imaging of upconverting nanophosphors in Caenorhabditis elegans," *Nano Letters*, vol. 6, no. 2, pp. 169–174, 2006.

[11] N. M. Idris, M. K. Gnanasammandhan, J. Zhang, P. C. Ho, R. Mahendran, and Y. Zhang, "*In vivo* photodynamic therapy using upconversion nanoparticles as remote-controlled nanotransducers," *Nature Medicine*, vol. 18, pp. 1580–1585, 2012.

[12] N. Menyuk, K. Dwight, and J. W. Pierce, "$NaYF_4$: Yb,Er—an efficient upconversion phosphor," *Applied Physics Letters*, vol. 21, no. 4, pp. 159–161, 1972.

[13] S. Heer, K. Kömpe, H. U. Güdel, and M. Haase, "Highly efficient multicolour upconversion emission in transparent colloids of lanthanide-doped $NaYF_4$ nanocrystals," *Advanced Materials*, vol. 16, no. 23-24, pp. 2102–2105, 2004.

[14] J. H. Zeng, J. Su, Z. H. Li, R. X. Yan, and Y. D. Li, "Synthesis and upconversion luminescence of hexagonal-phase $NaYF_4$:Yb, Er^{3+} phosphors of controlled size and morphology," *Advanced Materials*, vol. 17, no. 17, pp. 2119–2123, 2005.

[15] G. Yi, H. Lu, S. Zhao et al., "Synthesis, characterization, and biological application of size-controlled nanocrystalline $NaYF_4$:Yb,Er infrared-to-visible up-conversion phosphors," *Nano Letters*, vol. 4, no. 11, pp. 2191–2196, 2004.

[16] H.-X. Mai, Y.-W. Zhang, R. Si et al., "High-quality sodium rare-earth fluoride nanocrystals: controlled synthesis and optical properties," *Journal of the American Chemical Society*, vol. 128, no. 19, pp. 6426–6436, 2006.

[17] J.-C. Boyer, L. A. Cuccia, and J. A. Capobianco, "Synthesis of colloidal upconverting $NaYF_4$:Er^{3+}/Yb^{3+} and Tm^{3+}/Yb^{3+} monodisperse nanocrystals," *Nano Letters*, vol. 7, no. 3, pp. 847–852, 2007.

[18] J.-C. Boyer, F. Vetrone, L. A. Cuccia, and J. A. Capobianco, "Synthesis of colloidal upconverting $NaYF_4$ nanocrystals doped with Er^{3+}, Yb^{3+} and Tm^{3+}, Yb^{3+} via thermal decomposition of lanthanide trifluoroacetate precursors," *Journal of the American Chemical Society*, vol. 128, no. 23, pp. 7444–7445, 2006.

[19] Y. Wei, F. Lu, X. Zhang, and D. Chen, "Polyol-mediated synthesis and luminescence of lanthanide-doped $NaYF_4$ nanocrystal upconversion phosphors," *Journal of Alloys and Compounds*, vol. 455, no. 1-2, pp. 376–384, 2008.

[20] F. Zhang, Y. Wan, T. Yu et al., "Uniform nanostructured arrays of sodium rare-earth fluorides for highly efficient multicolor upconversion luminescence," *Angewandte Chemie*, vol. 46, no. 42, pp. 7976–7979, 2007.

[21] Y. J. Sun, Y. Chen, L. J. Tian et al., "Controlled synthesis and morphology dependent upconversion luminescence of $NaYF_4$:Yb, Er nanocrystals," *Nanotechnology*, vol. 18, no. 27, Article ID 275609, 2007.

[22] J. Zhao, Y. Sun, X. Kong et al., "Controlled synthesis, formation mechanism, and great enhancement of red upconversion luminescence of $NaYF_4$:Yb^{3+}, Er^{3+} nanocrystals/submicroplates at low doping level," *Journal of Physical Chemistry B*, vol. 112, no. 49, pp. 15666–15672, 2008.

[23] X. Wang, X. Kong, G. Shan et al., "Luminescence spectroscopy and visible upconversion properties of Er^{3+} in ZnO nanocrystals," *Journal of Physical Chemistry B*, vol. 108, no. 48, pp. 18408–18413, 2004.

[24] K. Yanagisawa and J. Ovenstone, "Crystallization of anatase from amorphous titania using the hydrothermal technique: effects of starting material and temperature," *Journal of Physical Chemistry B*, vol. 103, no. 37, pp. 7781–7787, 1999.

[25] D. Lin-Vien, N. B. Colthup, W. G. Fateley, and J. G. Grasselli, *The Handbook of IR and Raman Characteristic Frequencies of Organic Molecules*, Academic Press, New York, NY, USA, 1991.

[26] G. Socrates, *Infrared Characteristic Group Frequencies*, Wiley, New York, NY, USA, 2001.

[27] C. Burda, X. Chen, R. Narayanan, and M. A. El-Sayed, "Chemistry and properties of nanocrystals of different shapes," *Chemical Reviews*, vol. 105, no. 4, pp. 1025–1102, 2005.

[28] S. Kobayashi, K. Hiroishi, M. Tokunoh, and T. Saegusa, "Chelating properties of linear and branched poly(ethylenimines)," *Macromolecules*, vol. 20, no. 7, pp. 1496–1500, 1987.

[29] W.-J. Li, E.-W. Shi, and T. Fukuda, "Particle size of powders under hydrothermal conditions," *Crystal Research and Technology*, vol. 38, no. 10, pp. 847–858, 2003.

[30] H. Song, B. Sun, T. Wang et al., "Three-photon upconversion luminescence phenomenon for the green levels in Er^{3+}/Yb^{3+} codoped cubic nanocrystalline yttria," *Solid State Communications*, vol. 132, no. 6, pp. 409–413, 2004.

[31] A. M. Pires, O. A. Serra, and M. R. Davolos, "Morphological and luminescent studies on nanosized Er, Yb-yttrium oxide

up-converter prepared from different precursors," *Journal of Luminescence*, vol. 113, no. 3-4, pp. 174–182, 2005.

[32] A. M. Pires, S. Heer, H. U. Güdel, and O. A. Serra, "Er, Yb doped Yttrium based nanosized phosphors: particle size, "host lattice" and doping ion concentration effects on upconversion efficiency," *Journal of Fluorescence* , vol. 16, no. 3, pp. 461–468, 2006.